Received: 21 March 2021 | Revised: 16 May 2021 | Accepted: 17 May 2021

DOI: 10.1111/eci.13620

ORIGINAL ARTICLE

WILEY

Ga-68 EDTA aerosols in evaluation of inhaled-particle deposition and clearance of obstructive pulmonary diseases: A pilot prospective study compared with Galligas

Shao-Ting Wang[1] | **Cheng Bao**[1,2] | **Qingxing Liu**[3] | **Tengyue Zhang**[1] | **Yanli Yang**[1] | **Xinlun Tian**[1] | **Zhaohui Zhu**[3] | **Kai-Feng Xu**[1]

[1]Department of Pulmonary and Critical Care Medicine, State Key Laboratory of Complex Severe and Rare Diseases, Peking Union Medical College Hospital, Chinese Academy of Medical Sciences, Peking Union Medical College, Beijing, China

[2]Department of Pulmonary and Critical Care Medicine, Center of Respiratory Medicine, China-Japan Friendship Hospital, Beijing, China

[3]Department of Nuclear Medicine, State Key Laboratory of Complex Severe and Rare Diseases, Beijing Key Laboratory of Molecular Targeted Diagnosis and Therapy in Nuclear Medicine, Peking Union Medical College Hospital, Chinese Academy of Medical Sciences, Peking Union Medical College, Beijing, China

Correspondence
Kai-Feng Xu, Department of Pulmonary and Critical Care Medicine, Peking Union Medical College Hospital, Chinese Academy of Medical Sciences, Peking Union Medical College, #1 Shuaifuyuan Hutong, Beijing 100730, China.
Email: xukf@pumch.cn(KFX);

Zhaohui Zhu, Department of Nuclear Medicine, Peking Union Medical College Hospital, Chinese Academy of Medical Sciences, Peking Union Medical College, #1 Shuaifuyuan Hutong, Beijing 100730, China.
Email: zhuzhh@pumch.cn(ZZ)

Funding information
This work was supported by the National Key Basic Research Program of China (973 Program) (2015CB553402) and the National Key Research and Development Program of China (2018YFC1313600), and partly supported by the Chinese Academy of Medical Science Innovation Fund for Medical Sciences (2019-I2M-1-001), the Chinese Academy of Medical Science Clinical and Translational Medicine Research Foundation (2019XK320032), the National Natural Science Foundation of China (81871392) and the Capital Health Development Scientific Research Project (2018-1-4011)

Abstract

Purpose: 68-gallium (Ga-68) ethylenediaminetetraacetic acid (EDTA) aerosols and Galligas were compared in evaluation of inhaled-particle deposition and clearance in volunteers with or without obstructive pulmonary diseases.

Methods: Nonsmoking healthy volunteers, healthy smokers, asthma patients and patients with chronic obstructive pulmonary disease (COPD) were recruited to undergo the dynamic lung ventilation positron emission tomography/computerized tomography (PET/CT) scans within two consecutive days. The inhaled particles were Ga-68–labelled carbon nanoparticles (Galligas, 30-60 nm in size) and Ga-68–labelled EDTA aerosols (1-2 μm in size), respectively. The volunteers' lung function parameters were measured for comparison.

Results: Central deposition and inhomogeneity of both tracers were negatively correlated with lung function parameters, including the ratio of forced expiratory volume at 1 second to forced vital capacity (FEV_1/FVC). The central or hilum deposition of Galligas, but not 68-gallium (Ga-68) EDTA, was negatively correlated with the maximal expiratory flow at 25%, 50% and 75% of the forced vital capacity. Compared with Galligas, Ga-68 EDTA aerosols were more concentrated in the central region in all groups except for the healthy nonsmokers. Ventilation inhomogeneity was more evident when using Ga-68 EDTA aerosols, especially in patients with COPD and asthma patients. In the healthy smokers, the central region accumulated more Ga-68 EDTA at 30 minutes after inhalation than immediately after inhalation. Ga-68 EDTA cleared faster in lungs than Galligas.

Shao-Ting Wang, Cheng Bao and Qingxing Liu contributed equally to the manuscript.

Conclusions: Both Galligas and Ga-68 EDTA aerosols can be used for PET/CT lung ventilation scan. However, Ga-68 EDTA aerosols showed more advantages in diagnosis and evaluation of obstructive airway diseases by revealing the inhaled-particle deposition and clearance.

KEYWORDS

asthma, chronic obstructive pulmonary disease, Galligas, Ga-68 EDTA aerosol, PET/CT

1 | INTRODUCTION

Visualizing and quantifying the dynamic movement of inhaled particles in airways is critical for evaluation of airflow function and for investigation of the influence of particulate matter (PM) pollution as well. The complexity of airway structures makes it difficult to build a reliable model of deposition, distribution and clearance of inhaled PM. [1,2] The PM size and physiological conditions made the model even more complicated.[3-7] Studies of PM within human body are extremely limited because of difficulty in labelling and tracing.

Lung ventilation scintigraphy has been well established for mapping the deposition and clearance/translocation process of aerosol particles, allowing assessment of regional airflow function in a variety of diseases. In contrast, two-dimensional radionuclide scintigraphy and single photon emission computerized tomography (SPECT) with three-dimensional reconstructions can avoid the overlap of planar scintigraphy. However, it needs nearly 15 minutes for rotational acquisition for each time point, making it unsuitable for measuring deposition and clearance of radionuclide aerosols with fast clearance or translocation. Positron emission tomography (PET) can offer higher spatial resolution images and provide more accurate quantification. PET also allows more rapid acquisition when repeated measurements are required.[8]

Considering particle size may significantly contribute to the distribution and deposit of inhaled particles, we compared two positron emission tomography/computerized tomography (PET/CT) lung ventilation methods, using Ga-68–labelled carbon nanoparticles (Galligas) in 30-60 nm and Ga-68–labelled ethylenediaminetetraacetic acid (EDTA) aerosols in 1-2 μm, respectively. The two methods were compared in evaluation of airflow function and inhaled-particle deposition in the same groups of nonsmoking healthy volunteers, healthy smokers, asthma patients and patients with chronic obstructive pulmonary disease (COPD).

2 | METHODS

2.1 | Study population

The study protocol was reviewed and approved by the ethical committee of Peking Union Medical College Hospital, and all methods were carried out in accordance with relevant ethical guidelines and regulations, in compliance with the ethical principles of the Declaration of Helsinki. With written informed consent, 6 nonsmoking healthy volunteers, 7 healthy smokers, 4 asthma patients and 5 COPD patients (aged 20-65 years) were recruited to participate in this study.

All volunteers were referred for clinical assessment in the Department of Pulmonary and Critical Care Medicine in Peking Union Medical College Hospital. Before the recruitment, spirometry was measured using a Master Screen spirometer (CareFusion, Hoechberg, Germany). Pulmonary function parameters, including the ratio of forced expiratory volume at 1 second to forced vital capacity (FEV_1/FVC), were calculated; the maximal expiratory flow at 25%, 50% and 75% of the forced vital capacity was measured. All measurements were performed according to the standards established by the American Thoracic Society.[9]

The healthy volunteers had normal spirometry. The healthy nonsmokers were all never smokers, and the healthy smokers were current cigarette smokers with >10 pack-years smoking history. Exhaled breath carbon monoxide (eBCO) measurements using apiCO+Smokerlyzer® (Bedfont Scientific, England, UK) were performed in all subjects to verify smoking status. Agreement between eBCO threshold levels and self-reported cigarette smoking was certified by referring to previous study.[10]

Asthma patients were nonsmokers and met the diagnostic criteria of asthma by physicians.[11] Patients with COPD were restricted to those with spirometrically confirmed airflow obstruction (post-bronchodilator ratio of forced expiratory volume at 1 second to forced vital capacity (FEV_1/FVC) <0.7) and GOLD (Global Initiative for Chronic Obstructive Lung Disease) spirometric grade I-III (FEV_1 >30% predicted).[12]

Exclusion criteria included pregnancy, breastfeeding, symptoms of acute airway infections or exacerbation 4 weeks prior to the investigation, and history of malignancy, myocardial infarction, liver cirrhosis, renal failure and mental or intellectual disorders judged not able to provide informed consent. Reporting of the study conforms to broad EQUATOR guideline.[13]

2.2 | Galligas and Ga-68 EDTA preparation

Ga-68 was eluted using an on-site ^{68}Ge/Ga-68 generator (Eckert & Ziegler AG, Berlin, Germany) by 5 mL 0.05 mol/L hydrochloric acid, and 1 mL of Ga-68–labelled radiopharmaceuticals was chosen with highest radioactivity. Galligas was well-established radiotracer following the procedures of the Technegas Generator (Tetley Manufacturing Ltd., Sydney, Australia) and was buffered with acetate buffer to pH 7.0. To prepare Ga-68 EDTA aerosols, 5 mg EDTA was added into acetate buffer and suspension mixture was incubated for 10 minutes at 90°C. Labelling efficacy in excess of 95% was demonstrated by methanol: ammonium acetate performance control, and Ga-68 EDTA was inhaled as aerosol by using a nebulizer with gas flow rate of 7 L per minute. Galligas and Ga-68 EDTA aerosol used in this study represent two ranges of particle size, 30-60 nm and 1-2 μm, respectively.[14]

2.3 | PET/CT imaging

The PET/CT scanner was a Siemens Biograph 64 TruePoint System (Knoxville, Tennessee, USA). The inhalation procedures took place in a room separated from the PET/CT scanner to avoid any potential contamination, and the inhalation was performed when the patient was sitting in front of a gamma counter. The inhalation of Galligas and Ga-68 EDTA was terminated when the ventral count rate reached approximately 10 K and 50 K cps, respectively. After the inhalation, PET/CT scans were performed immediately in the supine position. The two PET/CT scans using Galligas and Ga-68 EDTA aerosols were performed in two consecutive days randomly. Low-dose axial CT was performed (140 kV, 35 mA, pitch 1:1, 3 mm thickness with 3 mm gap, 512 × 512 matrix, 70 cm field of view) from the neck to the upper abdomen for attenuation correction, followed by 5 lung ventilation PET acquisition (2 bed positions, 3 minutes each) for nearly 30 minutes (LR1 to LR5) to calculate lung retention.

2.4 | Image analysis

The PET/CT images were reviewed by 2 experienced physicians. The reconstructed PET/CT images were analysed in Fiji, an open-source image analysis platform.[15] The PET/CT Viewer plugin of Fiji with features of quantification was used in the subsequent analyses, and both airway and lung were included. Because the CT density ranges of the lung were close to those of air in the oesophagus or outside the body, the MorphoLibJ plugin of Fiji was used to reconstruct the three-dimensional structure of the respiratory system, and thus, the exact region of the respiratory system was defined.

Two methods, referred to as the 'central' method and the 'hilar' method, were introduced for evaluation of the particle distribution. (1)In the central method, a central area was defined inside a transverse CT plane and extended vertically along all planes containing lung to become a prismoid volume. Inside the prismoid volume, only airway and lung reconstructed by MorphoLibJ were included, which are the 'central' regions. As shown in Figure 1A, a quadrilateral (ALPR) was defined as central region on the transverse plane on the level of the carina of the trachea (Figure 1A). The central region was a three-dimensional volume. The volume and corresponding average standard uptake value (SUV) of the central region and those of the entire lungs were measured. The ratios of average SUV of the central region to the entire lungs were calculated. The inhomogeneity of particle distribution was also estimated using the ratio of maximal SUV to average SUV of the entire lungs.[16,17] (2)In the hilar method, 4 spheroid volumes of interest (VOI) were defined to investigate the characteristics of particle deposition at bifurcation of lobar bronchi. Firstly, the end of lobar bronchi was used as the centre of each VOI, and then, the radius was adjusted until the edge of VOI reaches the next bifurcation. Since the superior segmental bronchus of right lower lobe is adjacent to the right middle lobar bronchus, the right lower spheroid regions consist of the entry of both right middle lobe and right lower lobe. Thus, only four hilar spheroid regions were defined in this study. In addition, 4 corresponding subpleural regions were also determined by moving the previously defined hilar regions perpendicularly to sagittal plane across hilar spheroid centre until pleura, referring to as 'periphery' (Figure 1B). The average SUV and volume of each region were obtained. The sum of radioactivity of hilum spheroids divided by the sum of radioactivity of peripheral spheroids was considered as the indicator of hilum concentration.

For each individual, average SUV was measured in the 5 dynamic images (LR1 to LR5) separately. Clearance of inhaled radioactivity was estimated by calculating the decrease after 30 minutes. The proportion of initial activity remaining (retention ratio) after 30 minutes was measured by the ratio of average SUV in LR5 to that in LR1.

2.5 | Statistical analysis

Data were analysed using the R Project for Statistical Computing (v 3.5.2) software package (Lucent Technologies,

Murry Hill, New Jersey, USA) available at https://www.r-project.org/. Differences between multiple groups were evaluated by analysis of variance (Kruskal-Wallis) using the Dunnett test with the Bonferroni correction post hoc test and are presented as the mean ± SD. To explore the correlation between variables, Spearman's correlation (r) was used. Statistical significance was established at $P < .05$.

3 | RESULTS

3.1 | Central/hilum deposition and inhomogeneity of inhaled particles are correlated with airflow limitation

Twenty-two subjects with or without airflow limitation were recruited. The characteristics of those subjects are listed in Table 1. We defined central/hilum area of the lung as illustrated in Figure 1. Inhomogeneity was defined as the ratio of maximum SUV to mean SUV of the lung. As shown in Figure 2, there was a moderate negative correlation between the central deposition of Galligas (R = −0.53, $P = .01$) or Ga-68 EDTA (R = −0.54, $P = .0091$) and the ratio of FEV_1/FVC (Spearman's rank correlation test; Figure 2A, 2B). A moderate negative correlation between hilum deposition of Galligas (R = −0.76, $P = .000056$) or Ga-68 EDTA (R = −0.46, $P = .034$) and FEV_1/FVC was also observed (Figure 2C, 2D). Also, a moderate negative relationship between inhomogeneity for both particles and FEV_1/FVC was observed (Galligas, R = −0.57, $P = .0054$; Ga-68 EDTA, R = −0.66, $P = .00078$) (Figure 2E, 2F). Considering small airways, central or hilum Galligas deposition negatively correlated with maximal expiratory flow (MEF) after 25% (R = −0.53, $P = .012$; R = −0.67, $P = .0009$), 50% (R = −0.55, $P = .0096$; R = −0.58, $P = .0058$) and 75% (R = −0.46, $P = .032$; R = −0.53, $P = .011$) of FVC, while no similar results were proved with Ga-68 EDTA.

3.2 | Deposition patterns of 2 sizes of particles in different physiological conditions

We were able to investigate 2 sizes of particles that Figure 3 shows representative images from each different condition. Red area represents the particles, and the brightness is associated with local aggregation. Galligas (upper panel) produced

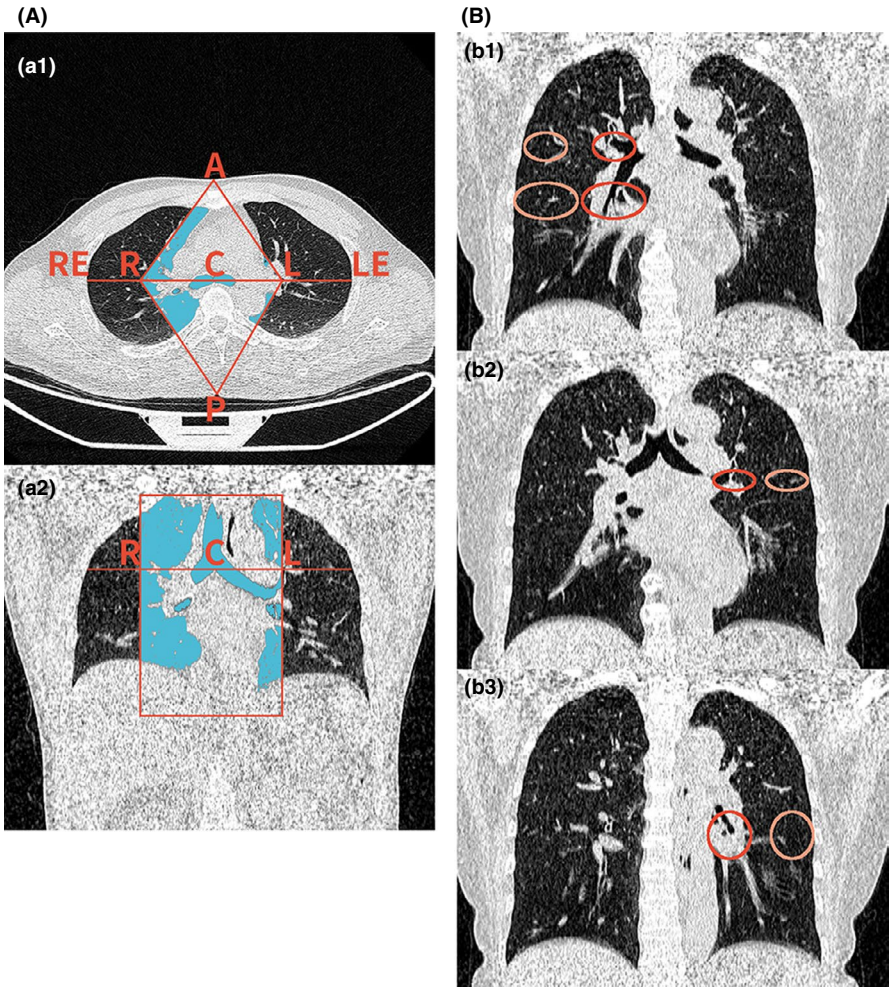

FIGURE 1 Definition of central area and hilar area in chest CT images. A, the central area was defined as a quadrilateral (ALPR) on the transverse plane on the level of the carina of the trachea(a1), with the four points at A: the anterior median line, P: the posterior median line, L: the midpoint of the carina (C) and the left edge of the lung(LE), and R: the midpoint of the carina (C) and the right edge of the lung (RE). 3D covering all transverse planes was calculated(a2). B, The hilar area was defined as four spheroid regions, of which the centres were located at the end of the right superior lobar bronchus and the end of bronchus intermedius(b1), the end of the left superior lobar bronchus(b2) and the end of left inferior lobar bronchus(b3). The radius of each spheroid region was determined by the linear distance between the centre and the next generation of bronchial bifurcation (red circles). Peripheral areas were determined by moving the spheroid regions laterally adjacent to pleura (orange circles)

brighter images than Ga-68 EDTA (lower panel) in all groups, indicating that smaller size facilitates deposition in distal airways. There is no patchy deposition of Galligas in healthy nonsmokers or smokers, and Galligas was able to reach distal airways in both groups. However, Ga-68 EDTA aerosols produced several hot areas in central airways in healthy smokers but not in nonsmokers. As for asthma and COPD groups, both particles aggregated in proximal airways. In particular, the 'cold zone' in marginal area of the COPD group shows the inadequate ventilation of distal airways in patients with COPD. The aggregations mentioned above mostly appeared in central airways before segmental bronchi.

Both physiological condition and particle size contributed to the deposition patterns of inhaled particles. Ga-68 EDTA aerosols were more concentrated in the central region than Galligas in all groups except for healthy nonsmokers (0 or 30 minutes after inhalation) (Figure 4A, 4B). Ga-68 EDTA aerosols concentrated more in the central region at 30 minutes compared with at 0 minutes only in healthy smoker group (30 minutes:1.13 ± 0.23 vs 0 minutes:1.03 ± 0.18, $P = .010$, paired t test). Among groups of Galligas or Ga-68 EDTA, there were no differences in inhomogeneity measure with the central area/total lung radioactive deposition ratio ($P > .05$, Kruskal-Wallis analysis of variance).

3.3 | Clearance is related to the size of the particle

Comparing radioactivity at 0 and 30 minutes on images, we were able to find the clearance of Ga-68 EDTA aerosol radiation seemed faster than Galligas in all groups, and the statistically significant difference in healthy nonsmokers and healthy smokers was observed, although they did not differ among the groups studied (Figure 5).

4 | DISCUSSION

Previously, a PET animal study demonstrated the applications of PET for investigating ultrafine particle inhalation.[18] The novelty of this report is that we firstly used a noninvasive quantitative approach with PET/CT ventilation scanning of the human lungs to improve our understanding of the dynamic distribution of inhaled particles in the airways. Functional status of large airways or small airways could be diagnosed or evaluated via imaging analysis of this approach. Advantages of this method are that the distribution, deposition and clearance of inhaled particles could be precisely traced, better than SPECT scan, a two-dimensional scan. PET/CT ventilation scan has potential in application of functional evaluation of complicated airways. As a PET/CT ventilation scan is used in clinical diagnostics, the accumulated data could potentially be used to generate an informative prediction of particle distribution in different physiological conditions while previously such information is hard to be obtained. The Dresden group in Germany previously used Ga-68 instead of Tc-99m to produce a radioaerosol feasible for PET imaging and compare such new technique with image using Tc-99m–labelled compounds.[19] In our study, we use PET/CT with Ga-68–labelled tracers for regional lung ventilation to yield regional lung deposition data in patients, which enables high-resolution pulmonary scintigraphy and quantitative evaluation. Additionally, Ga-68 is an ideal radiotracer for clinical use, with short half-life (68 minutes), on-site generator-based production, that enables more flexible imaging protocols compared with Tc-99m.

Several findings from this work are encouraging. (1) The work directly displayed that deposition patterns of inhaled fine and ultrafine particles were majorly determined by the degree of airflow limitation. In large airway, a low dense central deposition of both fine and ultrafine particles is related to FEV_1/FVC ratio, while in small airway, dense central deposition of ultrafine particles is related to a low MEF25, MEF50 or MEF75 value. Degree of inhomogeneity is also influenced by the degree of airflow limitation. In clinical practice, the PET/CT ventilation scan, inhaled either Ga-68 EDTA aerosols or Galligas, could be used as a novel method for diagnosis and evaluation of obstructive lung diseases. (2) In line of other reports, the 1-2 μm Ga-68 EDTA aerosols showed more central distribution than the 30-60 nm Galligas in different physiological airway conditions except in healthy nonsmokers.[20,21] (3) Different physiological conditions, with or without airway limitation, may play roles in determining the deposition and clearance of inhaled particles in varying degrees. It is a combined effect, determined not only by the particle sizes as we know previously, but also by different health conditions and pulmonary functions. Furthermore, the pulmonary function between individuals within the same group may vary. As an overall outcome, even similar pulmonary function test results may not mean the same airway status. For instance, a patient with unified moderate airway stenosis and another one with only several but severe stenosed bronchi may exert similar pulmonary function. Thus, PET/CT scan can provide airway status in detail.

We noticed that the relative concentration Ga-68 EDTA in central and hilum region increased in 30 minutes in the healthy smoker group compared with in 0 minutes. This result may indicate that cigarette smoke stimulates the function of tracheal/bronchial cilia and obtains higher clearance rate. An in vivo study proved that smokers manifested higher nasal mucociliary clearance times and nasal ciliary beat frequencies[22]; while other studies showed tobacco exposure resulted in less nasal ciliary beat frequency, or smoke or alcohol failed

TABLE 1 Characteristics of the study population

	Healthy nonsmokers (N = 6)	Healthy Smokers (N = 7)	Asthma (N = 4)	COPD (N = 5)	*P*-value
Age, years (range)	39.33 ± 6.86 (28-48)	35.0 ± 7.2 (28-50)	54.5 ± 10.8 (35-64)	61.2 ± 5.7[†] (58-63)	.003
Sex (M/F)	4/2	7/0	2/2	4/1	.265
BMI, kg/m^2	22.78 ± 1.48	22.30 ± 1.68	24.75 ± 3.26	23.69 ± 3.66	.702
Cigarette pack-year	0	24.98 ± 23.3	0	36.8 ± 27.5	.002
FEV_1 (%pred)	109.83 ± 15.24	104.67 ± 9.30	71.28 ± 22.06	53.04 ± 49.68[*,†]	.002
FEV_1/FVC, %	82.13 ± 2.64	82.02 ± 6.86	63.12 ± 13.32	49.78 ± 13.08[*,†]	.002
MEF25, %	77.87 ± 24.49	79.1 ± 15.48	31.08 ± 22.91	17.8 ± 8.33[*,†]	.003
MEF50, %	90.85 ± 17.02	86.83 ± 10.07	40.23 ± 25.73	22.54 ± 13.44[*,†]	.002
MEF75, %	107.98 ± 10.75	103.81 ± 15.25	53.5 ± 33.95	29.74 ± 20.34[*,†]	.003

Note: Data are expressed as the mean ± SD, and *P*-values were obtained by the Kruskal-Wallis test. Values in bold indicate significant differences ($P < .05$) by Dunnett's test with the Bonferroni correction.

*Patients with COPD versus healthy nonsmokers.

[†]patients with COPD versus healthy smokers.

to alter tracheal ciliary beat frequency but the combination could produce less ciliary beat frequency in mice. An in vitro study of human bronchial epithelium displayed that the extent and time of reduction in ciliary beat frequency depends on type of cigarette smoke.[23] Considering the paradoxical results in references, healthy smokers may be an independent group, not the state of transition of patients with COPD and healthy nonsmokers, and more subgroup studies, regarding the type of cigarette, the time of smoking and age, are required.

Previous studies have employed gamma scintigraphy (two-dimensional planar imaging) to understand the pulmonary deposition of inhaled aerosols. These studies utilized krypton (Kr81), xenon (Xe133) or cobalt (Co57) ventilation scan images to determine the outer boundary of the lung. The areas of the central and peripheral lung regions varied markedly among different methods for defining regions. The penetration index (PI, peripheral: central ratio normalized to a transmission lung scan), non-normalized parameters of the central/peripheral aerosol count ratio and the peripheral/central aerosol count ratio were reported to describe regional lung deposition.[24,25] Biddiscombe et al compared different indices among different methods for defining regions and found that PI, defined as peripheral/central aerosol counts normalized by peripheral/central krypton ventilation counts, was less affected by the size of the peripheral and central regions among different methods.[25] Using I-123 MIBG scintigraphy, Tomonobu et al found in patients with COPD the LMR (the total lung-to-upper mediastinum ratio) was not correlated with the pulmonary function parameters measured, including FEV_1, PaO_2, DL(CO) or pulmonary artery pressure at rest.[26]

Theoretically, larger particles tend to deposit at larger lumen. In this study, Ga-68 EDTA aerosols distributed more in central region, with different patterns among the different groups. Thus, Ga-68 EDTA aerosols are more suited for evaluation of trachea and bronchus, whereas Galligas is better to evaluate distal airways. In healthy subjects, expiratory flow limitation (EFL) does not occur during tidal breathing at rest. In previous study, time-activity curves of Technegas inhalation during 12 tidal breaths were measured in asthmatic subjects at control conditions and after exposure to inhaled methacholine. This study documented enhanced and spotty deposition of Technegas in the central lung regions with increasing radioactivity during tidal expiration.[27] We also noticed that in some patients, particles concentrated in smaller bronchi below segmental bronchi. Considering the variance of bronchial structure between subjects, high resolution of CT scan needs to be obtained with larger sample size.

The limitation of the study is the small sample size and that the definition of central areas and hilum is affected by body shape and bronchial tree variation, respectively. However, PET/CT ventilation scans will be a powerful method in evaluation of individuals under different physiological conditions.

5 | CONCLUSIONS

Deposition patterns of inhaled particles varied in different physiological airway conditions. Airflow limitation, defined as FEV_1/FVC ratio, determined distribution of inhaled particles. Ga-68 EDTA aerosols could be more suited for evaluation of tracheobronchial functions, whereas Galligas could

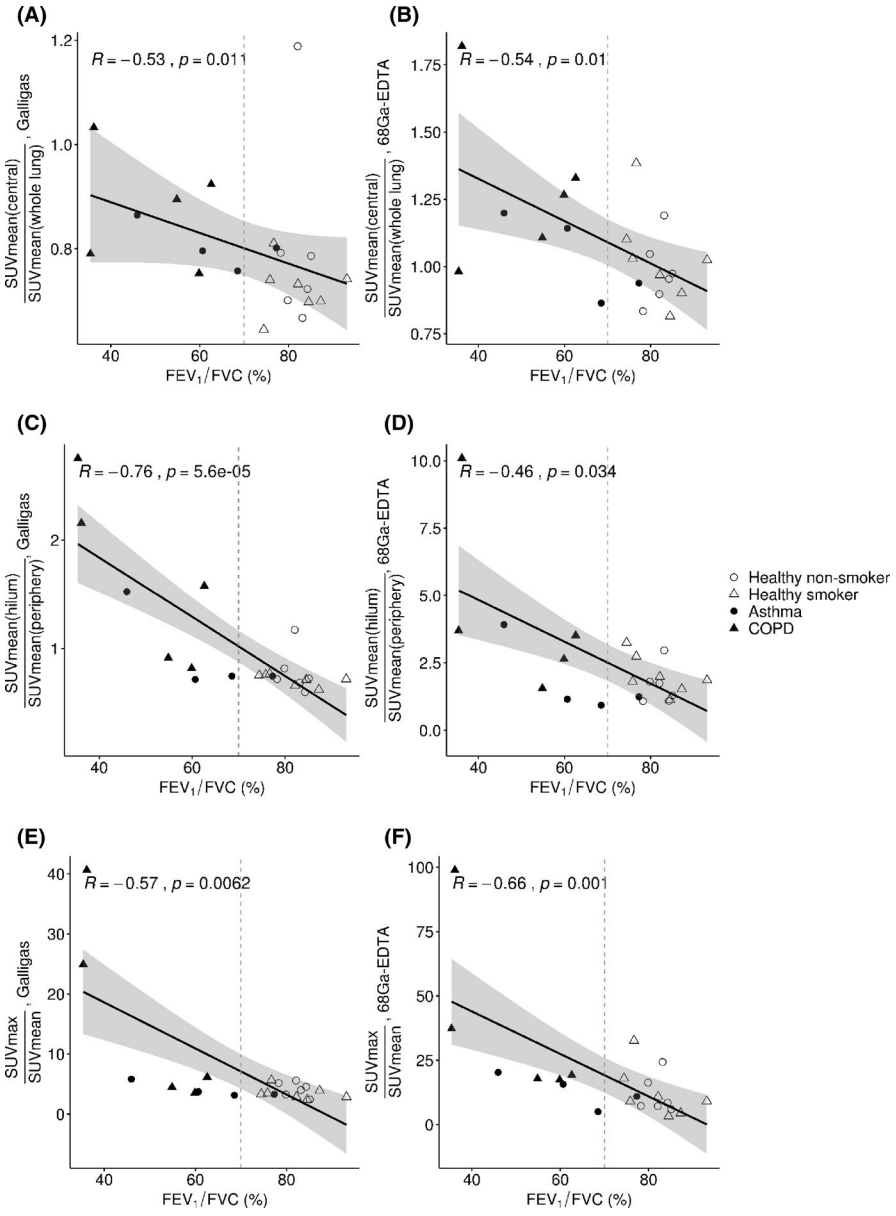

FIGURE 2 Central deposition and inhomogeneity of inhaled particles are correlated with airflow limitation. A, Central deposition of Galligas was correlated with FEV_1/FVC. B, Central deposition of Ga-68 EDTA was correlated with FEV_1/FVC. C, Hilar deposition of Galligas was correlated with FEV_1/FVC. D, Hilar deposition of Ga-68 EDTA was correlated with FEV_1/FVC. E, Inhomogeneity of Galligas was correlated with FEV_1/FVC. F, Inhomogeneity of Ga-68 EDTA was correlated with FEV_1/FVC

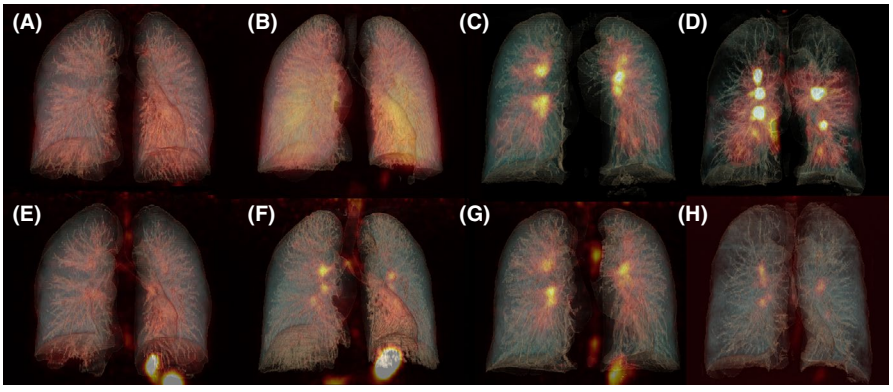

FIGURE 3 Diverse deposition patterns of Galligas and Ga-68 EDTA in airways under different physiological conditions. Coronal sections of PET/CT images of Galligas deposition of A, healthy nonsmokers, B, healthy smokers, C, asthma patients and D, patients with COPD and coronal sections of PET/CT images of Ga-68 EDTA aerosol deposition of E, healthy nonsmokers, F, healthy smokers, G, asthma patients and H, patients with COPD. Red areas indicate regions with the highest radioactivity, and black areas indicate the least radioactivity

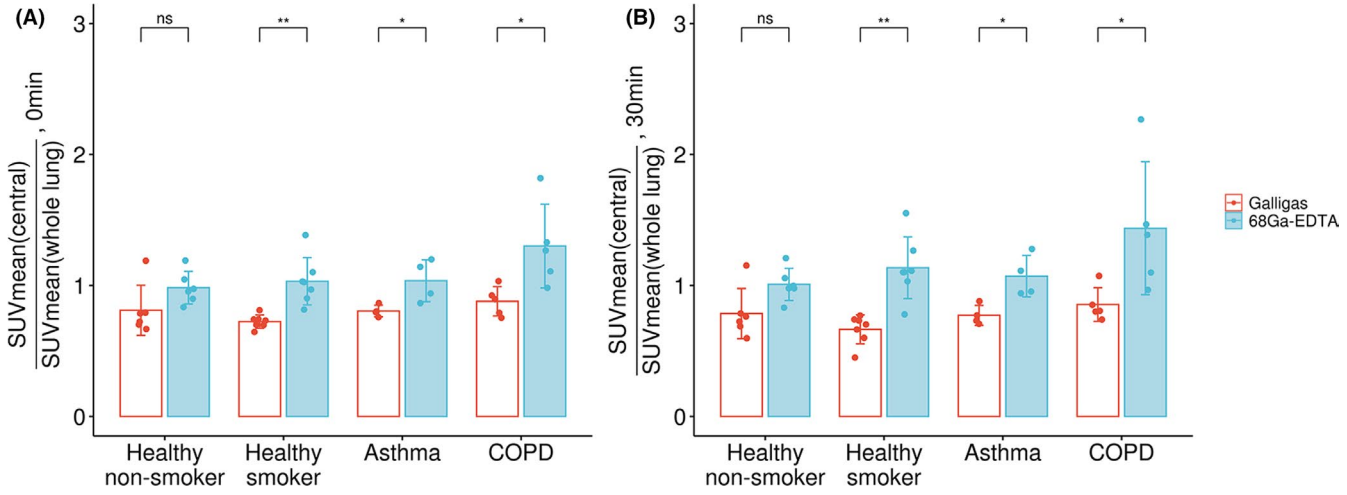

FIGURE 4 Central deposition at 0 min and 30 min after inhalation. A, Galligas produced less central deposition at 0-min healthy smokers, asthma patients and patients with COPD. B, Similar findings at 30 min after inhalation. * $P < .05$ and ** $P < .01$, paired t test

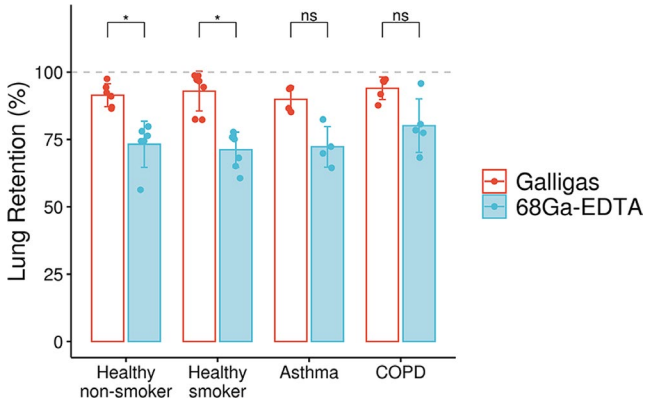

FIGURE 5 Particle retention at 30 min after inhalation. The lung retention (the ratio of LR5 to LR1 average SUV values) showed the clearance of Galligas was slower than Ga-68 EDTA in healthy nonsmokers and healthy smokers. * $P < .05$, paired Wilcoxon's test

be better to evaluate distal airways. Ga-68 PET/CT ventilation imaging is feasible and may be incorporated into clinical practice to evaluate airway functions.

ACKNOWLEDGEMENT

We thank Professor Li Wang from the Institute of Basic Medicine, Chinese Academy of Medical Sciences, for advice of the statistical analysis.

AUTHOR CONTRIBUTIONS

STW and CB contributed to patient recruitment, data analysis and writing of manuscript; QL and ZZ contributed to evaluation of PET/CT scan; TZ and YY contributed to clinical evaluation; ZZ and KFX contributed to design of the study, data analysis and writing of manuscript. All authors read and approved the final manuscript.

CONFLICTS OF INTEREST

The authors have no conflicts of interest to declare.

ETHICAL APPROVAL

The study protocol was reviewed and approved by the ethical committee of the Peking Union Medical College Hospital in December 2017 (JS-1493), and all methods were carried out in accordance with relevant ethical guidelines and regulations, in compliance with the ethical principles of the 1964 Declaration of Helsinki. The institutional review board for human studies approved the protocols, and written consent was obtained from all subjects.

DATA AVAILABILITY STATEMENT

All data generated or analysed during this study are included in this published article.

ORCID

Shao-Ting Wang https://orcid.org/0000-0001-8581-9899

REFERENCES

1. Churg A, Brauer M. Ambient atmospheric particles in the airways of human lungs. *Ultrastruct Pathol*. 2000;24:353-361.
2. Martonen TB, Schroeter JD, Hwang D, Fleming JS, Conway JH. Human lung morphology models for particle deposition studies. *Inhal Toxicol*. 2000;12(Suppl 4):109-121.
3. Fang D, Huang W, Antkiewicz DS, et al. Chemical composition and health risk indices associated with size-resolved particulate matter in Pearl River Delta (PRD) region, China. *Environ Sci Pollut Res Int*. 2019;26:12435-12445.
4. Gehring U, Beelen R, Eeftens M, et al. Particulate matter composition and respiratory health: the PIAMA Birth Cohort study. *Epidemiology*. 2015;26:300-309.
5. Eeftens M, Beelen R, de Hoogh K, et al. Development of Land Use Regression models for PM(2.5), PM(2.5) absorbance, PM(10) and

PM(coarse) in 20 European study areas; results of the ESCAPE project. *Environ Sci Technol*. 2012;46:11195-11205.
6. Lu Phuong N, Dang Khoa N, Inthavong K, Ito K. Particle and inhalation exposure in human and monkey computational airway models. *Inhal Toxicol*. 2018;30:416-428.
7. Dong J, Shang Y, Tian L, et al. Ultrafine particle deposition in a realistic human airway at multiple inhalation scenarios. *Int J Numer Method Biomed Eng*. 2019;35:e3215.
8. Hofman MS, Beauregard JM, Barber TW, et al. 68Ga PET/CT ventilation-perfusion imaging for pulmonary embolism: a pilot study with comparison to conventional scintigraphy. *J Nucl Med*. 2011;52:1513-1519.
9. Society AT. Lung function testing: selection of reference values and interpretative strategies. American Thoracic Society. *Am Rev Respir Dis*. 1991;144:1202-1218.
10. Al-Sheyab N, Kheirallah KA, Mangnall LJ, Gallagher R. Agreement between exhaled breath carbon monoxide threshold levels and self-reported cigarette smoking in a sample of male adolescents in Jordan. *Int J Environ Res Public Health*. 2015;12:841-854.
11. Global strategy for asthma management and prevention. *Workshop report 2018. Global Initiative for Asthma*. https://ginasthmaorg
12. Global Strategy for the Diagnosis, Management and Prevention of COPD(2017). *Global Initiative for Chronic Obstructive Lung Disease (GOLD)*. http://goldcopdorg.
13. Simera I, Moher D, Hoey J, Schulz KF, Altman DG. A catalogue of reporting guidelines for health research. *Eur J Clin Invest*. 2010;40:35-53.
14. Ament SJ, Maus S, Reber H, et al. PET lung ventilation/perfusion imaging using (68)Ga aerosol (Galligas) and (68)Ga-labeled macroaggregated albumin. *Recent Results Cancer Res*. 2013;194:395-423.
15. Schindelin J, Arganda-Carreras I, Frise E, et al. Fiji: an open-source platform for biological-image analysis. *Nat Methods*. 2012;9:676-682.
16. Zhao Z, Moller K, Steinmann D, Frerichs I, Guttmann J. Evaluation of an electrical impedance tomography-based Global Inhomogeneity Index for pulmonary ventilation distribution. *Intensive Care Med*. 2009;35:1900-1906.
17. Legland D, Arganda-Carreras I, Andrey P. MorphoLibJ: integrated library and plugins for mathematical morphology with ImageJ. *Bioinformatics*. 2016;32:3532-3534.
18. Palko HA, Fung JY, Louie AY. Positron emission tomography: a novel technique for investigating the biodistribution and transport of nanoparticles. *Inhal Toxicol*. 2010;22:657-688.
19. Kotzerke J, Andreeff M, Wunderlich G. PET aerosol lung scintigraphy using Galligas. *Eur J Nucl Med Mol Imaging*. 2010;37:175-177.
20. Usmani OS, Biddiscombe MF, Barnes PJ. Regional lung deposition and bronchodilator response as a function of beta2-agonist particle size. *Am J Respir Crit Care Med*. 2005;172:1497-1504.
21. Le Roux PY, Hicks RJ, Siva S, Hofman MS. PET/CT Lung Ventilation and perfusion scanning using Galligas and Gallium-68-MAA. *Semin Nucl Med*. 2019;49:71-81.
22. Stanley PJ, Wilson R, Greenstone MA, MacWilliam L, Cole PJ. Effect of cigarette smoking on nasal mucociliary clearance and ciliary beat frequency. *Thorax*. 1986;41:519-523.
23. Iskandar AR, Mathis C, Schlage WK, et al. A systems toxicology approach for comparative assessment: biological impact of an aerosol from a candidate modified-risk tobacco product and cigarette smoke on human organotypic bronchial epithelial cultures. *Toxicol In Vitro*. 2017;39:29-51.
24. Bennett WD, Brown JS, Zeman KL, et al. Targeting delivery of aerosols to different lung regions. *J Aerosol Med*. 2002;15:179-188.
25. Biddiscombe MF, Meah SN, Underwood SR, Usmani OS. Comparing lung regions of interest in gamma scintigraphy for assessing inhaled therapeutic aerosol deposition. *J Aerosol Med Pulm Drug Deliv*. 2011;24:165-173.
26. Koizumi T, Urushihata K, Hanaoka M, et al. Iodine-123 metaiodobenzylguanidine scintigraphic assessment of pulmonary vascular status in patients with chronic obstructive pulmonary disease. *Respirology*. 2010;15:1215-1219.
27. Pellegrino R, Biggi A, Papaleo A, et al. Regional expiratory flow limitation studied with Technegas in asthma. *J Appl Physiol*. 1985;2001(91):2190-2198.

How to cite this article: Wang S-T, Bao C, Liu Q, et al. Ga-68 EDTA aerosols in evaluation of inhaled-particle deposition and clearance of obstructive pulmonary diseases: A pilot prospective study compared with Galligas. *Eur J Clin Invest*. 2021;51:e13620. https://doi.org/10.1111/eci.13620